Journal of Alloys and Compounds 509 (2011) 9523–9527

Contents lists available at ScienceDirect

Journal of Alloys and Compounds

journal homepage: www.elsevier.com/locate/jallcom

Epitaxial growth of tin ferrite thin films using pulsed laser deposition technique

R.K. Gupta [a,*], F. Yakuphanoglu [b,c]

[a] Department of Physics, Astronomy, and Materials Science, Missouri State University, Springfield, MO 65897, USA
[b] Department of Physics, Firat University, Elazig 23169, Turkey
[c] Department of Physics and Astronomy, College of Science, King Saud University, Riyadh 11451, Saudi Arabia

ARTICLE INFO

Article history:
Received 17 April 2011
Received in revised form 15 July 2011
Accepted 18 July 2011
Available online 26 July 2011

Keywords:
Epitaxial thin films
$SnFe_2O_4$
Pulse laser deposition
Ferromagnetic
Bandgap

ABSTRACT

Epitaxial thin films of tin ferrite ($SnFe_2O_4$) were deposited on (0 0 2) oriented strontium titanate ($SrTiO_3$) substrate using pulsed laser deposition method. The quality and epitaxial nature of the films were investigated by X-ray diffraction technique. The phi scan of the film and the substrate shows four folds symmetry indicating cube-on-cube epitaxial growth of the film on the substrate. The optical bandgap of the film was estimated to be 2.6 eV using optical transmittance data. Magnetic measurements indicate that the coercive field and remnant magnetization of the film decrease with increase in temperature. The presence of hysteresis loop in *M vs. H* plot at room temperature indicates the ferromagnetic nature of the film.

1. Introduction

Spinel ferrites are very attractive magnetic materials because of their wide applications in magnetic devices, switching devices, ferrofluid technology and bio-medicals [1–4]. Spinels are generally denoted by the formula $(M^{II})_{\delta}(Fe^{III})_{1-\delta}[(M^{II})_{1-\delta}(Fe^{III})_{1+\delta}]O_4$, where the ions inside and outside the bracket occupy octahedral and tetrahedral sites, respectively. In this formula, when $\delta = 1$, it is called normal spinel. When $\delta = 0$, it is called an inverse spinel [5]. In spinel ferrites, tin ferrite ($SnFe_2O_4$) is a normal spinel with a cubic structure. Tin ferrite is an important candidate of the spinel family because of its technological importance [6,7]. Nanostructured spinel ferrites have been synthesized using different techniques such as sol–gel [8], co-precipitation [7], ball milling [9], combustion [10], solothermal polyol [11]. The influence of surface effect on the magnetic properties such as enhanced magnetization or superparmagnetism is observed in these nanostructured spinel ferrites [11].

For the miniaturization of complex geometrical devices, high quality films are required. It is observed that the saturation magnetizations of the bulk ferrites are higher than that of the films. Such change in the saturation magnetization of the bulk and film is due to formation of anti-boundary phase and possible disordered phase in the deposited films. In order to achieve high saturation magnetizations and avoid these detrimental factors, epitaxial growth of the film is desired [12]. The epitaxial thin films of various ferrites have been grown using variety of techniques [13–17]. Among these techniques, pulsed laser deposition technique (PLD) is a very versatile technique to deposit cost effective epitaxial thin films. PLD technique can produce films with quality comparable to molecular beam epitaxy (MBE) systems that cost 10 times as much and more [18].

Recently, Kim et al. [19] have deposited epitaxial thin films of magnesium ferrite on strontium titanate ($SrTiO_3$) substrate using PLD technique. The switching of magnetic anisotropy in epitaxial thin films of cobalt ferrite grown by PLD was studied [20]. Dix et al. [21] have studied the effect of substrate temperature on the film composition, morphology, and microstructure of bismuth ferrite–cobalt ferrite nanocomposites. Dhakal et al. [22] have studied the effect of substrate on the magnetic properties of cobalt ferrite films. Saturation magnetization of ~490 emu/cm^3 and ~300 emu/cm^3 was observed for the films grown on $SrTiO_3$ and MgO substrate, respectively. The observed difference was explained on the basis of lattice mismatch between substrate and film. There are few reports on the synthesis of nanostructured tin ferrite using different techniques [6,23,24] Lee et al. [25] have grown $Fe_{3-x}Mg_xO_4$ ferrite films on MgO and $SrTiO_3$ substrate that have the lattice mismatch of ~0.3% and ~7.5%, respectively with the ferrite. They observed that small lattice mismatch gives epitaxial films while large lattice mismatch produces relaxed films. Therefore, it would be interesting to optimize the growth conditions to fabricate epitaxial thin films of ferrites on large lattice mismatched substrates and study their properties. The literature survey indicates that there is no report on epitaxial growth of tin ferrite on

* Corresponding author. Tel.: +1 417 8366298; fax: +1 417 8366226.
E-mail address: ramguptamsu@gmail.com (R.K. Gupta).

0925-8388/$ – see front matter © 2011 Elsevier B.V. All rights reserved.
doi:10.1016/j.jallcom.2011.07.058

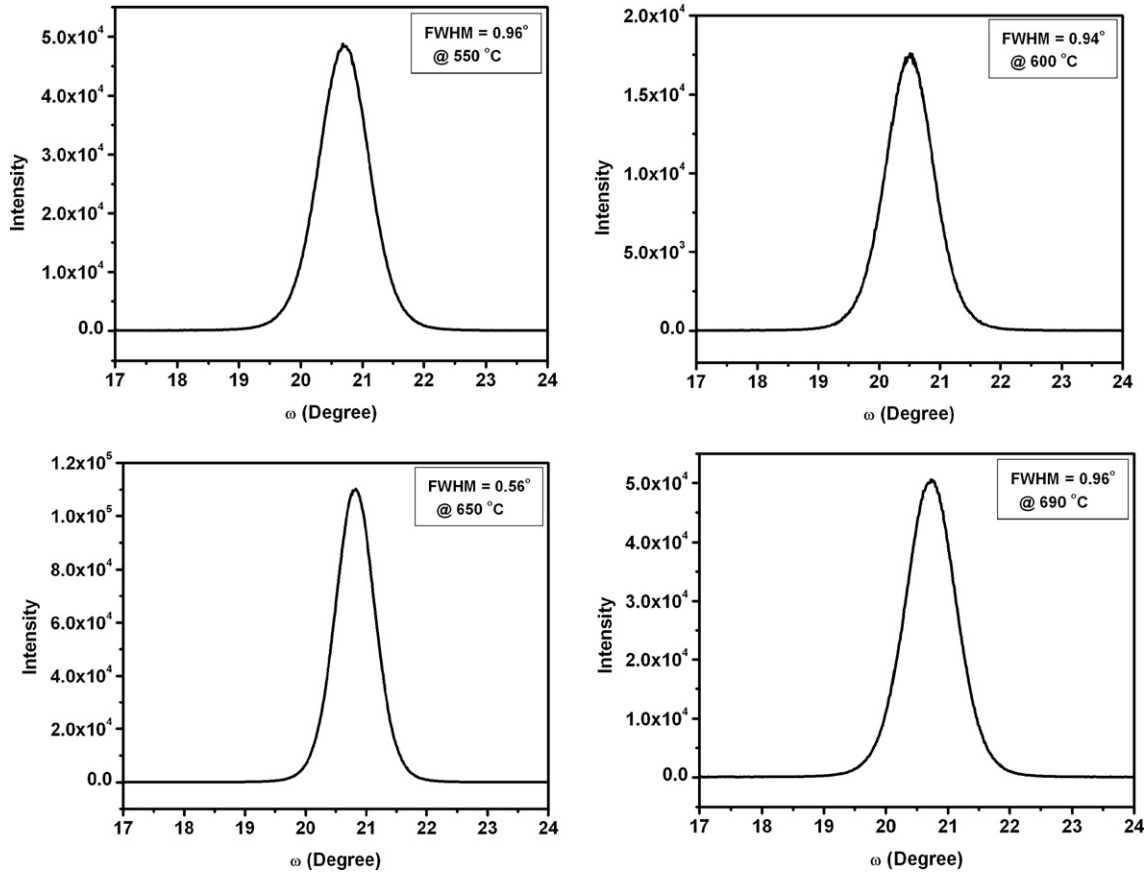

Fig. 1. Rocking curve (ω-scan) of the films grown at different temperatures.

$SrTiO_3$ substrate. In this paper, we report the fabrication and characterization of epitaxial thin films of $SnFe_2O_4$ using PLD. The detail structural, optical, electrical, and magnetic studies are presented in the following sections.

2. Experimental details

Solid state reaction method was used to prepare $SnFe_2O_4$ target using high purity SnO_2 and Fe_2O_3 (both from Alfa Aesar, USA). The well-ground mixture was heated at 1200 °C for 10 h. The powder mixture was cold pressed at 6×10^6 N/m^2 load and sintered at 1400 °C for 10 h. Pulsed laser deposition technique having KrF excimer laser (Lambda Physik COMPex, λ = 248 nm and pulsed duration of 20 ns) was used for deposition of the films. The film deposition using PLD can be divided into four steps: (1) laser interaction with the target; (2) ablation of target materials; (3) deposition of the ablated materials on the substrate; and (4) nucleation and growth of the film on the substrate surface. During the deposition of the films, the laser was operated at a pulse rate of 10 Hz, with an energy of 300 mJ/pulse. The laser beam was focused onto a rotating target at a 45° angle of incidence. The target was rotated with a constant speed to avoid erosion of a single spot. $SnFe_2O_4$ films were deposited at different growth temperature under oxygen pressure of 0.1 mbar on (0 0 2) oriented $SrTiO_3$ substrate.

The structural characterizations were performed using X-ray diffraction (XRD). The XRD spectra of the films were recorded with Bruker AXS X-ray diffractometer using the $2\theta-\theta$ scan, rocking curve, and phi scan using CuKα (λ = 1.5405 Å) radiation which operated at 40 kV and 40 mA. Quantum Design MPMS XL-T superconducting quantum interference device (SQUID) magnetometer was used to study the magnetic properties of the films.

3. Results and discussion

The X-ray diffraction technique was used to study the epitaxial nature of the films. It was observed that all the films have preferred orientation along (0 0 2) direction. Fig. 1 shows the rocking curve (ω-scan) for (0 0 2) peak of the films grown at different temperatures. The full width at half maximum (FWFM) of (0 0 2) peak was calculated. The FWFM was calculated to be 0.96°, 0.94°, 0.56°, and 0.96° for the films grown at 550 °C, 600 °C, 650 °C, and 690 °C, respectively. The lowest FWHM is observed for film grown at 650 °C, indicating highly quality of the film. We consider this high quality film for further characterizations. The X-ray diffraction pattern of the film grown at 650 °C is shown in Fig. 2(a). It is seen in the XRD pattern that only one peak oriented along (0 0 2) direction is observed, indicating the epitaxial nature of the film along (0 0 2) direction. These large lattice mismatched epitaxial thin films could be used to study the effect of strain and strain relaxation on the electronic and magnetic properties [26]. Both $SnFe_2O_4$ (face-centered cubic, $a = 0.839$ nm) and $SrTiO_3$ (primitive cubic, $a = 0.391$ nm) exhibit cubic symmetry. The phi (ϕ) scan of the film and substrate is shown in Fig. 2(b). The phi scan of the film and substrate reveal four folds symmetry for both. The phi scan shows a cube-on-cube epitaxial growth of $SnFe_2O_4$ on $SrTiO_3$ substrate.

Fig. 3 shows the optical transmittance spectra of the film. The optical bandgap of the film was calculated from absorption coefficient and photon energy. The absorption coefficient (α) was calculated using the expression [27].

$$\alpha = \frac{\ln(1/T)}{d} \quad (1)$$

where T is transmittance and d is film thickness. The optical bandgap of the films was calculated using equation [28]

$$(\alpha h\nu)^2 = A(h\nu - E_g) \quad (2)$$

where A and E_g are constant and optical bandgap, respectively. The E_g can be determined by extrapolations of the linear regions of the plot to zero absorption. Inset of Fig. 3 shows $(\alpha h\nu)^2$ *vs.* $h\nu$ plot for the film. The bandgap of the film was observed to be 2.6 eV. The observed bandgap is in good correlation with the other

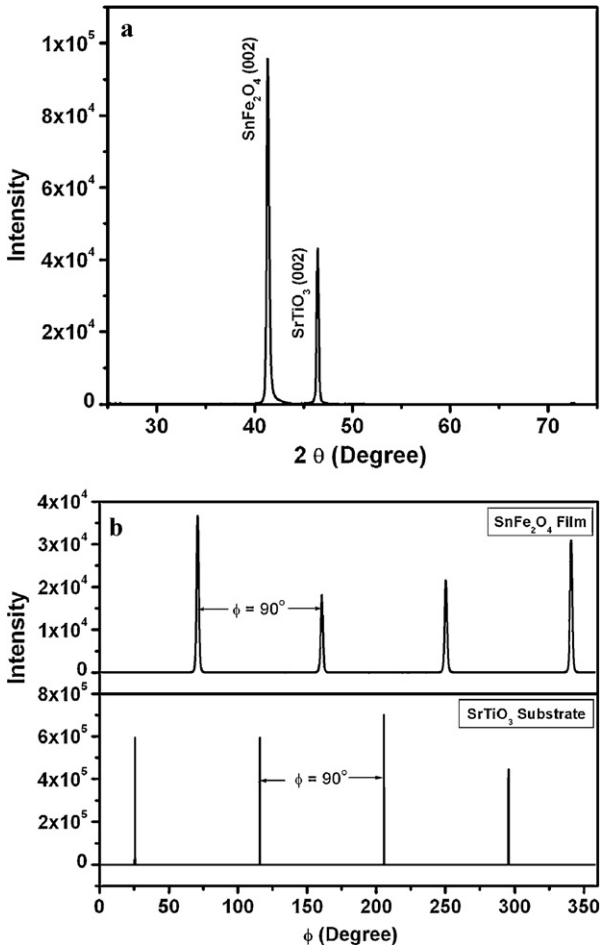

Fig. 2. XRD spectra of the $SnFe_2O_4$ film on $SrTiO_3$ substrate (a), phi (ϕ) scan of the $SnFe_2O_4$ and $SrTiO_3$ (b).

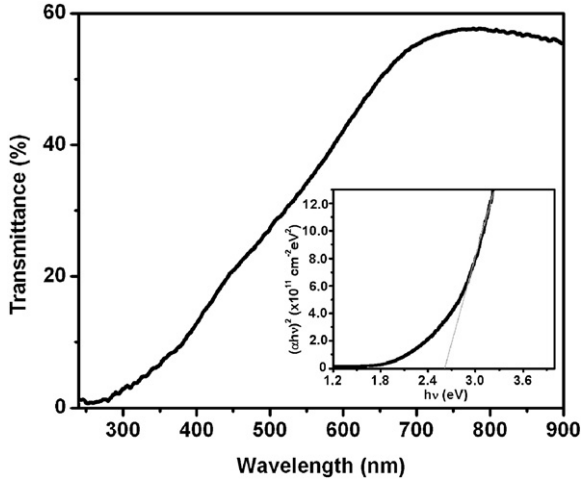

Fig. 3. UV–vis spectra of the film (inset figure shows $(\alpha h\nu)^2$ *vs.* $h\nu$ plot).

ferrites. For example, the optical bandgap of $NiFe_2O_4$ is reported as 2.5 eV [28]. Wu et al. [29] have reported the bandgap of spray pyrolysis deposited $ZnFe_2O_4$ as 2.7 eV. Benko and Koffyberg [30] have reported the bandgap of $MgFe_2O_4$ as 2.18 eV.

The temperature dependence resistivity measurement of the film shows semiconducting nature (Fig. 4). To better understand the transport mechanism, various electrical transport models such as hopping conduction and ionized impurity scattering were

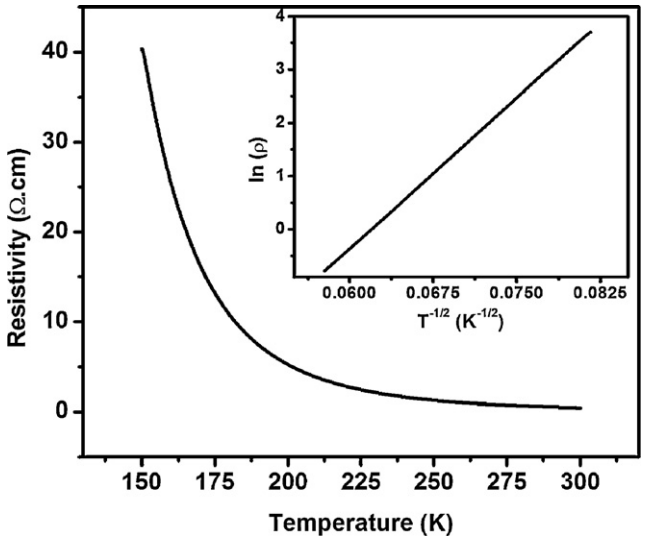

Fig. 4. Resistivity *vs.* temperature plot for the film (inset figure shows resistivity *vs.* (temperature)$^{-1/2}$ plot).

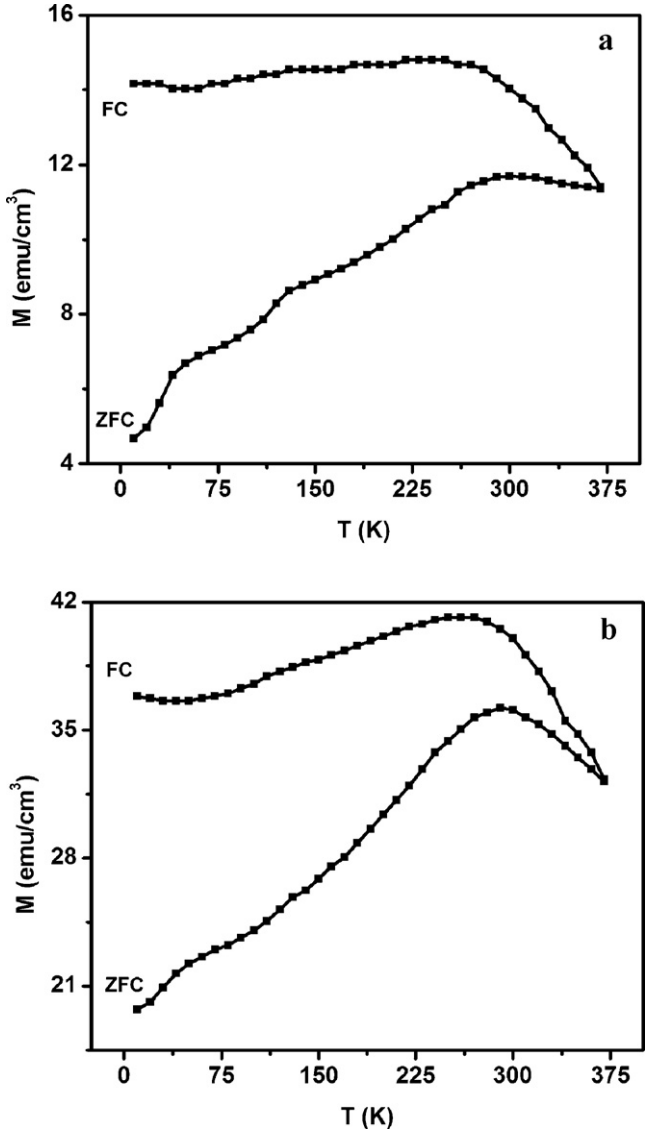

Fig. 5. *M vs. T* plots for $SnFe_2O_4$ film measured at (a) 500 Oe, and (b) 2000 Oe applied magnetic field.

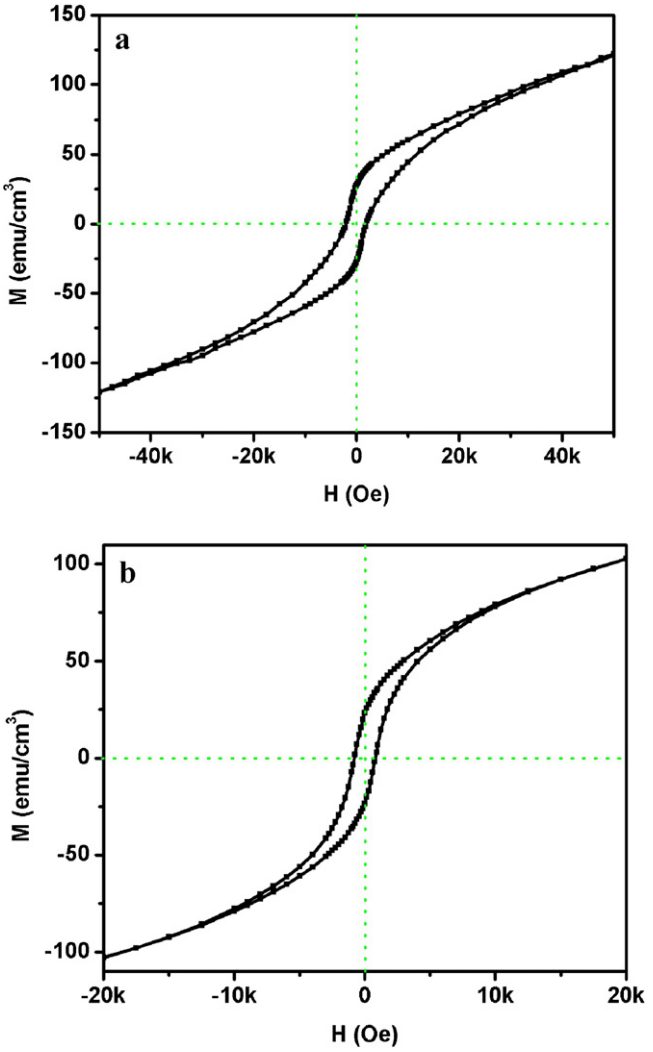

Fig. 6. *M vs. H* plots for $SnFe_2O_4$ film measured at (a) 10 K, and (b) 300 K.

considered. Hopping conduction is usually denoted by an equation of the form [31],

$$\rho(T) = B_1 \exp\left[\left(\frac{B_2}{T}\right)^{1/q}\right] \quad (3)$$

where T is the temperature. B_1, B_2 and q are constants and depend on conduction mechanism. For example, for variable range hopping conduction mechanism, $B_1 = AT^{1/4}$(A is independent of temperature) and $B_2 = 21/k_B g_n(\mu)\alpha^3$, where $g(\mu)$ is the density of the localized states, and α is the localization radius of charge carriers [32] $q = 1$ characterizes conduction dominated by hopping between localized states distributed in a periodic array (nearest neighbor hopping, NNH); $q = 4$ represents conduction between localized states distributed in a random array (variable range hopping, VRH). $q = 2$ is used for transportation of electrons through tunneling. For ionized impurity scattering, the temperature dependence of $\rho(T)$ is given by $\rho(T) \propto T^{-3/2}$. The data fits well for $q = 2$, indicates that the transport in the film is mainly due to tunneling. Lie et al. [33] have also observed the tunneling mechanism for zinc oxide doped Fe_3O_4.

Fig. 5 shows the effect of temperature on magnetization of $SnFe_2O_4$ film. The *M vs. T* data of the film was recorded at two different applied magnetic fields in zero-field-cooled (ZFC) and field-cooled (FC) process. For the ZFC measurements, the film was cooled from high temperature to 10 K without applying any external magnetic field. After cooling to 10 K, an external magnetic field was applied and the magnetization of the film was recorded as a function of temperature during heating. For FC measurements, the magnetization was recorded while cooling the sample under an applied external magnetic field. With increase in the temperature, magnetization increases up to ~300 K and decreases with further increase in the temperature. The nature of ZFC and FC curves is very similar but the magnitude of magnetization for FC curves is high. Also, it can be seen that the ZFC and FC magnetization curves show a distinct irreversibility behavior, and this irreversibility persists up to 375 K. Yamamoto et al. [34] have also reported the irreversibility behavior in ZFC and FC in *M vs. T* for $ZnFe_2O_4$ films.

The effect of external magnetic field on the magnetization of $SnFe_2O_4$ was studied at different temperatures. Fig. 6 shows the magnetization versus field (*M vs. H*) plots for $SnFe_2O_4$ film measured at 10 K and 300 K. It is clearly observable that these films are ferromagnetic at room temperature. As seen in Fig. 6, the coercive field and remnant magnetization of the film decrease with increase in the temperature. The coercive field of 1853 Oe and 801 Oe is observed at 10 K and 300 K, respectively. On the other hand, the value of remnant magnetization of 27 emu/cm^3 and 23 emu/cm^3 is observed at 10 K and 300 K, respectively. These epitaxial $SnFe_2O_4$ thin films could be used as a ferromagnetic component in magnetoelectric devices to enhance the coupling between ferromagnetic and ferroelectric and hence to get an optimal magnetoelectric properties [35].

4. Conclusions

Epitaxial thin films of $SnFe_2O_4$ were fabricated on $SrTiO_3$ substrate using pulsed laser deposition technique. The phi scan of the film and substrate shows four folds symmetry which confirms the cube-on-cube epitaxial growth of $SnFe_2O_4$ on $SrTiO_3$ substrate. The temperature dependence electrical measurement indicates the semiconducting nature of the film. Temperature and applied magnetic field studies indicate that $SnFe_2O_4$ film is ferromagnetic at room temperature.

Acknowledgements

RKG thankfully acknowledges National Science Foundation (DMR 0723105, DMR 0907037) and Missouri State University for providing research facilities and partial financial support.

References

[1] I. Bergmann, V. Šepelák, K.D. Becker, Solid State Ionics 177 (2006) 1865.
[2] P.P. Hankarea, U.B. Sankpal, R.P. Patil, I.S. Mulla, P.D. Lokhande, N.S. Gajbhiye, J. Alloys Compd. 485 (2009) 798.
[3] X. Xiang, G. Fan, J. Fan, F. Li, J. Alloys Compd. 499 (2010) 30.
[4] R.Y. Hong, J.H. Li, X. Cao, S.Z. Zhang, G.Q. Di, H.Z. Li, D.G. Wei, J. Alloys Compd. 480 (2009) 947.
[5] M.R. Anantharaman, S. Jagatheesan, K.A. Malini, S. Sindhu, A. Narayanasamy, C.N. Chinnasamy, J.P. Jacobs, S. Reijne, K. Seshan, R.H.H. Smits, H.H. Brongersma, J. Magn. Magn. Mater. 189 (1998) 83.
[6] O.N.C. Uwakweh, R.P. Moyet, R. Mas, C. Morales, P. Vargas, J. Silva, Á. Rossa, N. López, Phys.: J. Conf. Ser. 217 (2010) 012087.
[7] V.C.B. Pegoretti, P.R.C. Couceiro, C.M. Goncalves, M.F. Lelis, J.D. Fabris, J. Alloys Compd. 505 (2010) 125.
[8] B. Yang, Z. Li, Y. Gao, Y. Lin, C.W. Nan, J. Alloys Compd. 509 (2011) 4608.
[9] G.F. Goya, H.R. Rechenberg, Nanostruct. Mater. 10 (1998) 1001.
[10] Y.S. Zhang, G.C. Stangle, J. Mater. Res. 9 (1994) 1997.
[11] T.G. Altincekic, I. Boz, A. Baykal, S. Kazan, R. Topkaya, M.S. Toprak, J. Alloys Compd. 493 (2010) 493.
[12] H. Waqas, X.L. Huang, J. Ding, H.M. Fan, Y.W. Ma, T.S. Herng, A.H. Quresh, J.Q. Wei, D.S. Xue, J.B. Yi, J. Appl. Phys. 107 (2010) 09A514.
[13] H.C. Su, J.D. Dai, Y.F. Liao, Y.H. Wu, J.C.A. Huang, C.H. Lee, Thin Solid Films 518 (2010) 7275.
[14] G.W. Leung, M.E. Vickers, R. Yu, M.G. Blamire, J. Cryst. Growth 310 (2008) 5282.
[15] M. Zimnol, A. Graff, H. Sieber, S. Senz, S. Schmidt, R. Mattheis, D. Hesse, Solid State Ionics 101–103 (1997) 667.

[16] W. Huang, L.X. Zhou, H.Z. Zeng, X.H. Wei, J. Zhu, Y. Zhang, Y.R. Li, J. Cryst. Growth 300 (2007) 426.
[17] D. Reisinger, M. Schonecke, T. Brenninger, M. Opel, A. Erb, L. Alff, R. Gross, J. Appl. Phys. 94 (2003) 1857.
[18] S.M. Green, A. Pique, K.S. Harshavardhan, Pulsed Laser Deposition of Thin Films, Wiley, New York, 1995 (chapter 2).
[19] K.S. Kim, P. Muralidharan, S.H. Han, J.S. Kim, H.G. Kim, C. Cheon, J. Alloys Compd. 503 (2010) 460.
[20] X.S. Gao, D.H. Bao, B. Birajdar, T. Habisreuther, R. Mattheis, M.A. Schubert, M. Alexe, D. Hesse, J. Phys. D: Appl. Phys. 42 (2009) 175006.
[21] N. Dix, R. Muralidharan, J.M. Caicedo, D. Hrabovsky, I. Fina, L. Fabrega, V. Skumryev, M. Varela, J. Guyonnet, P. Paruch, F. Sanchez, J. Fontcuberta, J. Magn. Magn. Mater. 321 (2009) 1790.
[22] T. Dhakal, D. Mukherjee, R. Hyde, P. Mukherjee, M.H. Phan, H. Srikanth, S. Witanachchi, J. Appl. Phys. 107 (2010) 053914.
[23] F. Liu, T. Li, H. Zheng, Phys. Lett. A 323 (2004) 305.
[24] F.X. Liu, T.Z. Li, Mater. Lett. 59 (2005) 194.
[25] D.S. Lee, J.S. Wang, D.K. Modak, Y.S. Liu, C.L. Chang, G. Chern, J. Appl. Phys. 101 (2007) 09M523.
[26] Y. Suzuki, Annu. Rev. Mater. Res. 31 (2001) 265.
[27] V.R. Shinde, T.P. Gujar, C.D. Lokhande, R.S. Mane, S.H. Han, Mater. Chem. Phys. 96 (2006) 326.
[28] S.N. Dolia, R. Sharma, M.P. Sharma, N.S. Saxena, Ind. J. Pure Appl. Phys. 44 (2006) 774.
[29] Z. Wu, M. Okuya, S. Kaneko, Thin Solid Films 385 (2001) 109.
[30] F.A. Benko, F.P. Koffyberg, Mater. Res. Bull. 21 (1986) 1183.
[31] J. Ederth, P. Johnsson, G.A. Niklasson, A. Hoel, A. Hultaker, P. Heszler, C.G. Granqvist, A.R. van Doorn, M.J. Jongerius, Phys. Rev. B 68 (2003) 155410.
[32] E. Arushanov, S. Siebentritt, T.S. Niedrig, M.C.L. Steiner, J. Appl. Phys. 100 (2006) 063715.
[33] C.T. Lie, P.C. Kuo, W.C. Hsu, I.J. Chang, J.W. Chen, J. Magn. Magn. Mater. 239 (2002) 160.
[34] Y. Yamamoto, H. Tanaka, T. Kawai, J. Magn. Magn. Mater. 261 (2003) 263.
[35] H. Zheng, J. Wang, S.E. Lofland, Z. Ma, L.M. Ardabili, T. Zhao, L.S. Riba, S.R. Shinde, S.B. Ogale, F. Bai, D. Viehland, Y. Jia, D.G. Schlom, M. Wuttig, A. Roytburd, R. Ramesh, Science 303 (2004) 661.